ASTRONOMY & ASTROPHYSICS
SUPPLEMENT SERIES

Astron. Astrophys. Suppl. Ser. **117,** 449-465 (1996)

CCD spectrophotometry of CVs. III. 3270−9000 Å atlas for 38 faint systems⋆

T. Zwitter[1] and U. Munari[2]

[1] University of Ljubljana, Department of Physics, Jadranska 19, 1000 Ljubljana, Slovenia
E-Mail: tomaz.zwitter@uni-lj.si
[2] Osservatorio Astronomico di Padova, Sede di Asiago, I-36032 Asiago (VI), Italy
E-Mail: munari@astras.pd.astro.it

Received October 23; accepted November 29, 1995

Abstract. — A 7 Å resolution, 3270−9000 Å spectrophotometric atlas is presented for 38 objects from the Downes & Shara (1993) catalogue of Cataclysmic Variables (CVs). The stars were selected among those listed as lacking published spectra. As for previous papers in this series, the aim is to check the CV status of the objects spectroscopically and to provide high quality absolute spectrophotometry over a wide wavelength range. For all programme stars accurate $UBVRI$ magnitudes, continuum fluxes at selected wavelengths and integrated fluxes of emission lines are derived. Among the 38 programme stars, only 16 clearly show a CV–like spectrum. In the three papers of this series we have so far surveyed 94 objects among the entries in the Downes and Shara catalogue which lack spectroscopic confirmation. The fraction of validated CVs is 56%. For objects from the Palomar–Green survey the rate of confirmed CVs is particularly low, amounting to only 23%.

Key words: stars: cataclysmic variables — white dwarfs — atlases

1. Introduction

Downes & Shara (1993, hereafter DS93) have compiled a very useful catalogue and atlas of the Cataclysmic Variables discovered through February 1992. A similar work for classical novae was presented by Duerbeck (1987, hereafter D87). DS93 listed references to published quiescence spectra for 271 objects and to outburst spectra for additional 123 systems (in both cases a significant fraction belonging to the *pre-digital* era), but for 359 objects (∼half of the total) they have been unable to locate published spectra.

In Papers I and II of this series (Zwitter & Munari 1994, 1995) we have begun to present CCD spectra for CVs listed by DS93 as lacking published spectroscopy.

The results of Papers I and II confirm the conclusion of DS93 and D87 that the classification of an object as a CV using exclusively the information from photometric observations and/or automated spectral surveys may be misleading. The large fraction of misclassifications we have encountered so far supports the need for a spectroscopic survey to prune the excellent DS93 catalogue from mis-entries. A cleaned version of the DS93 CV list is the basic requirement for investigations like those involving cross-checks with catalogues of sources in various spectral domains (γ−ray, X–ray, EUV, radio, ...), and for careful planning of precious observing time with orbiting satellites and large ground–based telescopes.

In this paper we present flux-calibrated CCD spectra for additional 38 southern faint systems selected among those without published quiescence spectra according to the DS93 catalogue. The programme continues and observations of additional targets will be presented in future papers of this series.

Beside the confirmation of the CV status, our spectra are intended to expand the set of validated CVs with high quality and flux calibrated spectra. A physical analysis of spectral charateristics (emission lines, continuum slope, etc.) is postponed to a final paper in this series.

2. Observations

A journal of the observations is given in Tables 1 and 2. Cited parameters of the programme stars are from DS93.

The observations have been performed with the B&C + CCD spectrograph at the 1.50 m ESO telescope. We used a 400 l/mm grating and a 2 arcsec slit, resulting in a resolution of 7 Å and a wavelength range $\lambda\lambda$ 3270−

Send offprint requests to: T. Zwitter
⋆Based on observations collected with the telescopes of the European Southern Observatory at La Silla, Chile

Table 1. Journal of observations of the programme stars. Type, Max and Min as listed by DS93. Code for spectral information available in literature (DS93): N = no spectral information; D = only a glass plate tracing or a description of the quiescence spectrum; X = only a glass plate tracing or a description of the outburst spectrum. Status of the object when we have observed it: Q = quiescence; Out = outburst

Name	$\alpha_{2000.0}$	$\delta_{2000.0}$	Type	Max (mag)	Min (mag)	Code	Observ. date	UT (mid-exp)	Expt. time	Status
MV Gem	07 00 53.37	+12 51 16.3	UG	15.3 p	17 p	D	20.04.95	01 07	45^{min}	Q
DY Pup	08 13 48.40	–26 33 57.1	nb:	7.0 p	20 p	N	18.04.95	23 56	45^{min}	Q
VZ Pyx	08 59 19.95	–24 28 55.7	dq	12.5 V	16.8 V	N	20.04.95	23 52	30^{min}	Q
PG 0911-066	09 14 14.09	–06 47 45.6	cv	14.2 B		D	17.04.95	23 54	30^{min}	Q
PG 0947+036	09 49 40.41	+03 24 24.1	cv	16.8 B		N	22.04.95	02 51	27^{min}	Q
V411 Car	10 31 19.24	–59 58 25.7	n	14.5 p	19 p	X	23.04.95	00 18	45^{min}	Q
CN Vel	11 02 40	–54 23 11	nb	10.2 p	17 :p	X	18.04.95	01 26	45^{min}	Q
V365 Car	11 03 15.98	–58 27 27.5	nb	10.1 p	21.6 j	X	22.04.95	00 59	45^{min}	Q
PG 1119+147	11 22 13.15	+14 26 20.6	cv	16.1 B		N	23.04.95	01 39	60^{min}	Q
MU Cen	12 12 53.92	–44 28 17.1	ugSS	11.8 p	15.0: p	D	20.04.95	04 14	30^{min}	Q
CG Mus	12 20 13.74	–74 13 16.0	UGZ	15.9 p	17.0 p	N	19.04.95	00 57	45^{min}	Q
V373 Cen	12 26 05.19	–45 49 31.9	ug	13.5 p	15.8 p	D	18.04.95	02 49	40^{min}	Q
BM Cha	13 08 06.84	–77 55 06.0	ug:	14.6 B	16.6 B	N	19.04.95	01 43	30^{min}	Q
NN Cen	13 14 15.66	–60 52 47.0	UGSS	13.2 p	17.5 p	N	19.04.95	03 41	40^{min}	Q
PG 1314+041	13 16 38.54	+03 48 17.2	cv	15.9 B		N	20.04.95	02 22	45^{min}	Q
RR Cha	13 26 23.44	–82 19 43.4	na	7.1 p	19.3 j	N	23.04.95	03 22	60^{min}	Q
GY Hya	14 30 30.54	–25 52 39.1	ug:	14 p	16 p	N	18.04.95	03 54	30^{min}	Q
PG 1459-026	15 02 12.22	–02 45 59.1	cv	15.0 B		N	18.04.95	04 39	40^{min}	Q
PG 1520-050	15 23 18.63	–05 11 44.2	cv	15.3 B		N	21.04.95	05 04	45^{min}	Q
AG Aps	15 30 22.43	–75 44 39.4	UG	14.3 p	>16.0 p	N	19.04.95	04 40	45^{min}	Q
V699 Oph	16 25 22.65	–04 40 25.3	ug	13.8 p	18.5 p	N	22.04.95	03 54	45^{min}	Q
V422 Ara	16 59 19.08	–61 43 33.9	UG	14.2 p	16.2 p	N	19.04.95	06 23	45^{min}	Q
V478 Sco	17 25 58.55	–35 32 32.3	UG	14.0 B	16.7 B	N	18.04.95	06 14	40^{min}	Q
V972 Oph	17 34 43.81	–28 10 35.8	nb	8.0 p	17.0 j	D	18.04.95	07 04	40^{min}	Q
V2493 Sgr	18 00 40.93	–29 00 12.8	UG:	15.4 p	17.1 p	N	18.04.95	09 06	20^{min}	Q
KY Ara	18 08 12.29	–54 54 22.3	ug:	15.1 p	18 :p	N	19.04.95	08 46	30^{min}	Q
UZ Ser	18 11 24.96	–14 55 34.9	ugSS	11.9 v	16.0 v	D	23.04.95	05 31	45^{min}	Out
V3909 Sgr	18 14 22.04	–27 51 06.7	UG:	15.5 p	16.6 p	N	20.04.95	08 24	30^{min}	Q
V3914 Sgr	18 14 49.07	–30 43 29.8	UG:	14.1 p	>16.0 p	N	20.04.95	09 02	30^{min}	Q
WW Tel	18 23 56.84	–54 59 39.0	UG	14.6 p	18.5 p	N	23.04.95	07 30	45^{min}	Q
V4019 Sgr	18 25 27.41	–25 40 08.1	NL:	13.0 p	15.0 p	N	19.04.95	09 34	30^{min}	Q
DP Pav	18 26 42.85	–64 59 31.5	ug:	15.0 p	>16.5 p	N	19.04.95	07 30	30^{min}	Q
YY Tel	18 33 56.43	–53 58 51.1	ugwz:	14.4 p	>17.4 p	N	21.04.95	07 56	45^{min}	Q
BP CrA	18 36 50.88	–37 25 53.8	ugz	13.5 v	15.9 v	D	23.04.95	06 35	45^{min}	Q
BD Pav	18 43 12.03	–57 30 45.2	ug	12.4 p	16.5 j	D	23.04.95	08 22	45^{min}	Q
V2038 Sgr	18 45 20.52	–26 27 48.3	UG:	14.0 p	16.2 p	N	20.04.95	09 35	20^{min}	Q
NSV 11561	18 56 34.16	–08 35 30.4	n::	16.2 p	17.0 p	N	23.04.95	09 17	45^{min}	Q
V1089 Sgr	19 08 48.07	–17 21 38.3	UGSS	13.8 p	17 :p	N	18.04.95	09 37	40^{min}	Q

Table 2. Target objects without recorded spectra because at the time of our observations they were too faint. Type, Max and Min as listed by DS93. The scheme for spectral code (from DS93) is the same as in Table 1. Last column: magnitude of the object as estimated on the screen of the CCD guiding system of the B&C spectrograph at the ESO 1.5 m telescope

Name	$\alpha_{2000.0}$	$\delta_{2000.0}$	Type	Max (mag)	Min (mag)	Code	UT observ. date	V (mag)
RX Cha	10 36 27.03	–80 02 52.4	UG	14.4 p	>16.9 p	N	Apr 22.018 1995	≥ 20.5
V812 Cen	13 13 54.18	–57 40 44.5	n	11 p	18 j	X	Apr 21.055 1995	≥ 20.0

Table 3. Classification of the programme stars

Name	Classification	Name	Classification	Name	Classification
MV Gem	mid–F dwarf	NN Cen	confirmed CV	UZ Ser	confirmed CV
DY Pup	confirmed CV	PG 1314+041	B subdwarf	V3909 Sgr	M3 III (Mira ?)
VZ Pyx	confirmed CV	RR Cha	confirmed CV	V3914 Sgr	Mira (M7)
PG 0911-066	confirmed CV	GY Hya	confirmed CV	WW Tel	G0 V
PG 0947+036	WD (DA type)	PG 1459-026	M2 V	V4019 Sgr	A7e
V411 Car	K1–2 III: e:	PG 1520-050	O subdwarf	DP Pav	A2–3 V
CN Vel	confirmed CV	AG Aps	confirmed CV	YY Tel	hot continuum
V365 Car	confirmed CV	V699 Oph	K	BP CrA	confirmed CV
PG 1119+147	late B	V422 Ara	A V + K7 V	BD Pav	confirmed CV
MU Cen	confirmed CV	V478 Sco	confirmed CV	V2038 Sgr	Mira (M4)
CG Mus	F3 V	V972 Oph	confirmed CV	NSV 11561	K4 V
V373 Cen	confirmed CV	V2493 Sgr	Mira (M3)	V1089 Sgr	K3–5 III
BM Cha	T Tau	KY Ara	F7 V		

9000 Å. The slit was always rotated perpendicularly to horizon in order to minimize problems connected with differential atmospheric refraction. All details on observing strategy, data reduction, seeing and spectrophotometric standards are identical to those described in Paper II.

Atmospheric extinction and instrumental response have been derived individually for each observing night. Intercomparison of the standard stars throughout the whole observing run shows that mean rms error of the absolute flux calibration does not exceed 4% over the $\lambda\lambda 3450-8700$ Å wavelength range. Outside these bounds the flux calibration error degrades appreciably.

3. Results

The flux calibrated spectra for the programme stars are presented in Figs. 4-19. Some spectra have been misplaced for plot clarity: the shift in ordinate units is given in brackets after the star name. An asterisk before the star name indicates that a boxcar smoothing (with a window of 3 pixels) has been applied to increase the visibility of faint features in spectra with low S/N ratio.

3.1. *Classification of programme stars*

The classification of the programme stars is given in Table 3. Following the criterium adopted in Papers I and II, we consider a programme star as a *spectroscopically confirmed CV* if the contemporaneous presence of emission lines and a hot continuum can be traced in the recorded spectrum. In addition, the relative intensity of emission lines should conform to that of the template CV spectrum shown in Fig. 1 of Paper II. The only exceptions to this rule are UZ Ser (which was in outburst when we observed it) and old novae (see indivudal notes below).

3.2. *Emission lines and continuum fluxes*

The integrated absolute fluxes of the most prominent emission lines are given in Table 4. No correction for reddening has been applied. A parabolic fit of the underlying continuum over a 100 Å range has been used for each line.

Continuum fluxes at the same selected wavelengths as in Papers I and II are given in Table 5 for each programme star. They have been averaged over 50 Å bins.

3.3. *UBVRI magnitudes and colours*

The V magnitude and the $U-B$, $B-V$, $V-R_{\rm C}$ and $R_{\rm C}-I_{\rm C}$ colours have been computed from the flux calibrated spectra of each object. The values are listed in Table 6. They are primarily intended for statistical use and to improve or fill in the missing photometric entries in the DS93 catalogue. For the band transmission profiles we have used the same sources as adopted in Papers I and II: Lamla (1982; Vilnius Observatory reconstruction) for U and B, and Bessell (1976) for V, $R_{\rm C}$ and $I_{\rm C}$.

The error level of the magnitudes and colours has been estimated by a comparison of derived and tabulated values for each standard star calibrated against all the other ones observed during the same night. The error matches the one listed above for the absolute flux calibration. A somewhat larger value is however to be expected for the programme stars because their recorded spectra have in general a lower signal–to–noise ratio. The accuracy of the V magnitudes for objects fainter than V=18 probably degrades further for two reasons: optimal placing on the slit of very faint targets may be problematic and the CCD could not respond in a linear way to very low photon fluxes.

However, when photoelectric or CCD photometry for any of the targets is found in literature, the difference with our derived $UBVR_{\rm C}I_{\rm C}$ data is remarkably small, rarely exceeding 0.1 mag even in the problematic U band (see

Table 4. Integrated flux (in units of 10^{-15} erg cm^{-2} s^{-1}) of the most prominent emission lines

	Hα	Hβ	Hγ	Hδ	He I (4471 Å)	He I (5876 Å)	He I (6678 Å)	He I (7065 Å)	He II (4686 Å)
DY Pup	0.3								
VZ Pyx	139	155	170	137	35.6	31.3	15.2	10.0	18.8
PG 0911-066	3.6								
CN Vel	0.9								
V365 Car	1.4								
MU Cen	78.7	57.8	75.3	49.3		6.9			
V373 Cen	16.1	11.7	12.2	9.1		2.5	2.0:		
BM Cha	651	33.8	11.4	7.6		12.0	9.1		
NN Cen	14.6	10.2	8.6	6.3	2.5	3.3	1.1	1.4:	
RR Cha	5.7	1.8	1.0			0.9	0.6	0.6:	1.6
GY Hya	113	79.1	69.8	56.5	13.3	11.3	10.5	5.8:	83.4
AG Aps	13.5	12.1	9.4	7.0	3.2:	3.2	1.2		
V478 Sco	18.1	11.0	7.4	4.4		2.7	1.2		
V972 Oph	4.9	2.5:							
UZ Ser	27	15							
V3914 Sgr			24.8	55.9					
V4019 Sgr	116	2.0:							
BP CrA	51.9	41.4	41.4	31.1	10.0	10.7	2.5	2.5	
BD Pav	43	23				10	9.5	8.1	
V2038 Sgr			3.5:	10.8					

individual notes below). Given the intrinsic variability of the objects under investigation which adds up to this difference, we may state that for the bulk of the targets the V magnitudes are accurate to 0.10 mag, the $U-B$ colour to 0.10 mag and $B-V$, $V-R_{\rm C}$, $R_{\rm C}-I_{\rm C}$ colours to 0.05 mag.

In Figs. 1 and 2 the colours of the programme stars are compared with the entries in the UBV photometric catalogue of CVs by Bruch & Engel (1994, hereafter BE94) and with the values of confirmed CVs from Papers I and II.

The confirmed CVs from the present paper well overlap those from Papers I and II and the CVs from BE94 in both colour diagrams suggesting consistent and accurate calibration procedures. On the average, the validated CVs in this paper suffer from a greater reddening than those studied in Paper II.

3.4. *Hα profiles*

In Fig. 3 the Hα profiles of the confirmed CVs are plotted on an expanded scale. The profile of the night–sky line at 5577.4 Å in the spectrum of NN Cen is shown as a template of the instrumental resolution (NN Cen being one of the CV with the narrower Hα profile). It is evident in Fig. 3 how our spectra can resolve the gross profile structure of the emission lines (cf. Paper II).

4. Notes on individual objects

4.1. *Confirmed cataclysmic variables*

DY Pup. This is Nova Pup 1902, the faintest target we observed. Szkody (1994) reported V=19.1, $B-V$=+0.1 and $V-R$=+0.2 with errors of the order of 0.2 mag. Such values are in good agreement with our findings in Table 6 (taking also into account the intrinsic variability of the object). Our spectrum shows a blue continuum with a moderate Hα in emission.

VZ Pyx. Our spectrum looks identical to that in quiescence reported by Remillard et al. (1994), except for a bluer slope of the continuum. Our photometry in Table 6 is in excellent agreement with the photoelectric photometry reported by Remillard et al.

CN Vel is the East component of the faint optical double on the finding chart in D87. It is Nova Vel 1905. On our spectrum we measured B=18.0, which would set the outburst amplitude to 8 mag. Only Hα is seen in emission on a blue continuum.

V365 Car. The emission line He II 4686 Å is much stronger than Hβ and no He I line is detectable. This suggests extreme temperature for the hot component. The interstellar reddening may contribute to the relatively red slope of the continuum, the object being quite faint and on the galactic equator ($b=+1^\circ$).

MU Cen, **V373 Cen**, **V478 Sco** and **BP Cra**. The UBV values measured on our spectra and reported in

Table 5. Continuum fluxes for the programme stars. The fluxes have been scaled to Flux (5200 Å) = 1.00. They were computed averaging over 50 Å wide bins centered at the given wavelength

Name	Continuum Fluxes										
	3450	3750	4000	4400	4800	5200	5600	6000	7050	8000	8800
MV Gem	0.39	0.49	0.86	0.99	1.04	1.00	1.00	0.98	0.83	0.71	0.62
DY Pup			1.47	1.23	1.24	1.00	0.84	0.78	0.53	0.42	
VZ Pyx	2.19	2.05	1.29	1.06	1.03	1.00	0.94	0.90	0.80	0.65	0.50
PG 0911-066	1.83	1.68	1.39	1.18	0.95	1.00	0.81	0.70	0.48	0.31	0.27
PG 0947+036	4.15	3.25	2.50	1.83	1.27	1.00	0.78	0.61	0.36	0.13	
V411 Car	0.32	0.34	0.63	0.77	1.04	1.00	1.05	1.12	1.01	0.96	0.86
CN Vel			1.42	1.20	1.11	1.00	0.89	0.76	0.53	0.39	0.34
V365 Car	1.06	1.00	0.97	0.98	0.98	1.00	1.00	0.99	0.95	0.87	1.01
PG 1119+147	2.68	2.25	2.04	1.61	1.25	1.00	0.81	0.70	0.47	0.33	0.27
MU Cen	1.20	1.12	0.97	0.96	1.04	1.00	1.06	1.07	0.96	0.86	0.73
CG Mus	0.07	0.25	0.52	0.75	0.94	1.00	1.05	1.06	0.95	0.86	0.76
V373 Cen	1.09	1.06	0.99	0.96	1.07	1.00	1.07	1.08	0.98	0.87	0.77
BM Cha	0.03	0.12	0.15	0.40	0.73	1.00	1.56	2.05	3.33	4.59	5.41
NN Cen			1.11	0.98	0.98	1.00	0.99	1.07	1.32	1.50	
PG 1314+041	2.92	2.26	2.04	1.59	1.26	1.00	0.84	0.72	0.49	0.36	0.27
RR Cha			0.27	0.59	0.79	1.00	1.15	1.11	1.17	0.62	0.93
GY Hya	1.40	1.37	1.03	1.03	1.02	1.00	1.00	0.99	0.87	0.73	0.58
PG 1459-026			0.14	0.64	0.89	1.00	1.64	1.91	3.32	4.68	4.77
PG 1520-050	3.69	2.85	2.42	1.76	1.30	1.00	0.79	0.63	0.38	0.24	0.17
AG Aps		1.22	1.32	1.06	1.12	1.00	1.07	1.00	0.97	0.87	0.80
V699 Oph	0.20	0.25	0.35	0.65	1.09	1.00	1.37	1.53	1.52	1.39	1.36
V422 Ara			1.14	1.16	1.09	1.00	0.97	1.00	0.90	0.91	0.98
V478 Sco	1.24	1.18	1.05	1.05	1.01	1.00	1.03	1.01	0.96	0.90	0.86
V972 Oph	0.64	0.75	0.66	0.79	0.87	1.00	1.19	1.28	1.42	1.53	1.61
V2493 Sgr				0.38	0.63	1.00	1.74	2.18	5.36	9.17	11.3
KY Ara	0.50	0.63	0.87	0.94	1.07	1.00	1.02	1.01	0.81	0.69	0.63
UZ Ser	1.37	1.32	1.41	1.26	1.12	1.00	0.92	0.81	0.60	0.47	0.39
V3909 Sgr		0.03	0.08	0.37	0.66	1.00	1.83	2.24	5.76	9.37	11.2
V3914 Sgr					0.57	1.00	1.70	2.90	16	41	134
WW Tel	0.60	0.65	0.88	1.00	1.07	1.00	1.10	1.01	0.82	0.73	0.63
V4019 Sgr	0.37	0.71	0.85	0.88	0.97	1.00	1.09	1.10	1.04	1.01	0.97
DP Pav	0.52	0.70	1.21	1.18	1.14	1.00	0.95	0.88	0.66	0.54	0.49
YY Tel	0.71	1.07	1.15	1.11	1.16	1.00	0.90	0.95	0.73	0.48	0.55
BP CrA	1.84	1.77	1.25	1.11	1.02	1.00	0.97	0.96	0.92	0.83	0.70
BD Pav	0.58	0.59	0.78	0.99	1.18	1.00	1.17	1.22	1.10	0.94	0.78
V2038 Sgr				0.55	0.89	1.00	1.69	2.42	10.4	23	107
NSV 11561	0.11	0.17	0.35	0.57	0.94	1.00	1.23	1.35	1.34	1.30	1.26
V1089 Sgr	0.17	0.26	0.44	0.69	1.00	1.00	1.17	1.21	1.13	1.04	0.97

Table 6 are in excellent agreement with the photometry listed by Bruch (1984) and BE94.

NN Cen is marked as the West component of a close optical pair in the finding chart of DS93. That component itself is however a pair in the N-S direction with $\sim 3.5''$ separation. The CV is the faint northern component of the pair. The cool southern component which is brighter in the red makes the flux calibration of the red part of our spectrum uncertain.

RR Cha is Nova Cha 1953. On our well exposed spectrum we measured B=20.1, which sets the outburst amplitude to $\triangle B$=13.0 mag. The star shows pronunced He II emission (almost comparable to Hβ). Together with V972 Oph it is the hottest post–nova we have observed.

V972 Oph. It is Nova Oph 1957. We measured B=17.5 (cf. Table 6) which sets the outburst amplitude to $\triangle B$=9.5 mag. The He II 4686 Å is in strong, double–peaked emission, while Hβ emission is weaker, narrow and visible inside a background, wide absorption. The contemporaneous absence of emission in He I lines suggests that the WD has an extremely high temperature. Together with RR Cha it is the hottest post–nova we have observed. The continuum is markedly red in slope. The absence of TiO and Mg b in absorption suggests an F–type or earlier continuum, in which case the reddening from Table 6 may

Table 6. $U-B$, $B-V$, $V-R_C$, R_C-I_C colour indices and V magnitude for the programme stars as derived from our absolute spectrophotometry

Name	V	$U-B$	$B-V$	$V-R_C$	R_C-I_C	Name	V	$U-B$	$B-V$	$V-R_C$	R_C-I_C
MV Gem	17.53	+0.34	+0.67	+0.37	+0.49	AG Aps	18.06	–0.41	+0.51	+0.40	+0.59
DY Pup	19.63	–0.72	+0.27	+0.16		V699 Oph	18.38	+0.81	+1.18	+0.60	+0.73
VZ Pyx	15.14	–1.03	+0.37	+0.35	+0.48	V422 Ara	17.20		+0.50	+0.38	+0.73
PG 0911-066	18.92	–0.84	+0.21	+0.12	+0.13	V478 Sco	16.48	–0.56	+0.57	+0.43	+0.67
PG 0947+036	17.47	–1.16	–0.23	–0.05		V972 Oph	16.56	–0.26	+0.98	+0.63	+0.91
V411 Car	17.66	+0.41	+0.91	+0.47	+0.66	V2493 Sgr	15.80			+1.23	+1.73
CN Vel	17.78	–0.54	+0.29	+0.16	+0.23	KY Ara	16.26	+0.04	+0.70	+0.35	+0.49
V365 Car	18.31	–0.51	+0.63	+0.43	+0.67	UZ Ser	13.55	–0.54	+0.30	+0.20	+0.32
PG 1119+147	16.99	–0.91	–0.01	+0.07	+0.14	V3909 Sgr	14.27		+2.07	+1.22	+1.72
MU Cen	14.73	–0.59	+0.64	+0.44	+0.60	V3914 Sgr	14.83		+1.56	+2.06	+2.54
CG Mus	16.61	+0.95	+0.94	+0.44	+0.60	WW Tel	18.16	+0.02	+0.67	+0.37	+0.48
V373 Cen	16.27	–0.52	+0.66	+0.43	+0.60	V4019 Sgr	14.44	+0.05	+0.78	+0.49	+0.70
BM Cha	14.58	+1.32	+1.81	+1.09	+1.35	DP Pav	14.71	+0.11	+0.44	+0.25	+0.38
NN Cen	18.11	–0.86	+0.51	+0.60	+1.00	YY Tel	19.26	–0.28	+0.47	+0.30	+0.30
PG 1314+041	15.89	–0.96	+0.01	+0.10	+0.19	BP CrA	16.11	–0.90	+0.43	+0.42	+0.64
RR Cha	18.93			+0.53	+0.40	BD Pav	15.12	+0.05	+0.78	+0.45	+0.56
GY Hya	15.08	–0.66	+0.51	+0.39	+0.51	V2038 Sgr	16.33		+1.53	+1.86	+2.51
PG 1459-026	17.68		+1.58	+0.95	+1.43	NSV 11561	14.14	+1.05	+1.29	+0.60	+0.76
PG 1520-050	15.84	–1.09	–0.16	–0.02	–0.05	V1089 Sgr	15.74	+0.74	+1.10	+0.51	+0.65

amount to as much as E_{B-V}=0.5, in agreement with the strength of the Na I D absorption line and the very low galactic latitude of the object ($b = +2°$).

UZ Ser. The comparison of our photometry with the quiescence and outburst values listed by BE94 suggests that we caught the object in outburst, quite close to the maximum. This is confirmed by the spectral appearance: wide and shallow absorption lines with a broad emission core.

BD Pav. It is also known as Nova Pav 1934. On our quiescence spectrum we measured B=15.9 which would set the outburst amplitude to a mere $\triangle B$=3.5 mag. Our UBV values in Table 6 are in good agreement with the photometry reported by BE94. The continuum is that of an early K star, with very strong Na I D and Mg b absorptions. The absence of He II and presence of He I emission suggest the hot component to be hot though cooler than the old novae RR Cha and V972 Oph. Barwing & Schoembs (1983) performed a thorough analysis of BD Pav. They suggest it not to be a classical nova but more likely a dwarf nova with rare outbursts and long term spectroscopic variations. Their 1980 spectrum shows a higher excitation and stronger hot continuum compared with our one in Fig. 10.

4.2. *Other objects*

MV Gem. Bond (1978) reported the star to show a "blue continuum with wide, shallow hydrogen absorption lines, typical of a U Gem variable near maximum light" on plate spectra obtained at dispersions 210−240 Å/mm. Our spectrum has a dispersion of 180 Å/mm but the hydrogen lines look quite sharp (compare with the spectrum of UZ Ser in outburst in Fig. 16). The spectral type could be that of a mid–F dwarf. The star is found to be in B band about one magnitude fainter than the reported range of variability, which is consistent with the results in Paper I.

V411 Car. Known as Nova Car 1953, it was discovered by Perek (1960) as an emission line object on two objective prism plates secured in February and March 1953. Duerbeck (1984) reported about inspection of Harvard patrol plates: the star was not visible in 1952, in January 1953 it was at m_{pg}=14.5 and two months later it had faded to m_{pg}=17.0. We find the object now to be at B=18.6 (Table 6) and to show a K1–2 (possibly luminosity class III) absorption continuum. The Hα could have a weak emission component on both sides of the central absorption (separation between the peaks $\sim$ 900 km s^{-1}). The nature of the object is not clear.

BM Cha. The spectrum presented in Fig. 3 shows very weak TiO absorption bands consistent with a K7 V classification. The emission lines of H I (Balmer and Paschen series), infrared Ca II triplet and He I suggest the object to be a young stellar object. It lies in the direction of Chamaeleon II star forming region. The T Tau classification from objective prism plates of Hartigan (1993) is confirmed.

PG 1314+041. The presence of He I and lack of He II absorptions suggest a classification as B subdwarf, the object laying at galactic latitude $b = +66°$.

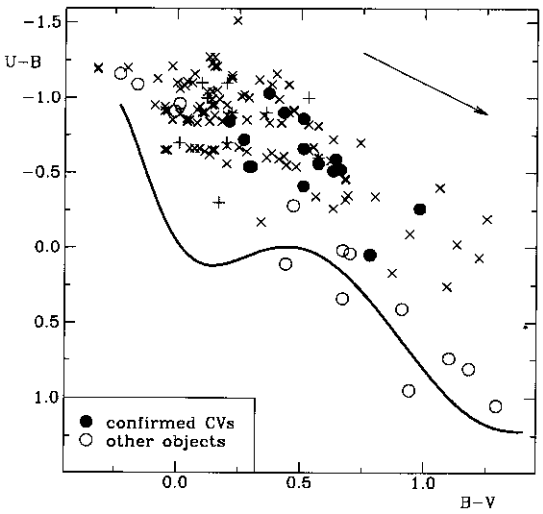

Fig. 1. $U-B$, $B-V$ diagram of programme stars. No reddening correction has been applied to the data given in Table 6. The reddening vector corresponding to E_{B-V}=0.5 is shown. The solid line is the ZAMS according to Caldwell et al. (1993). Legend: *filled circles* = confirmed CVs from the present paper; *open circles* = other programme stars; *crosses* = CVs in quiescence from the UBV photometric catalogue of Bruch & Engel (1994); *plus signs* = validated CVs in quiescence from Paper II

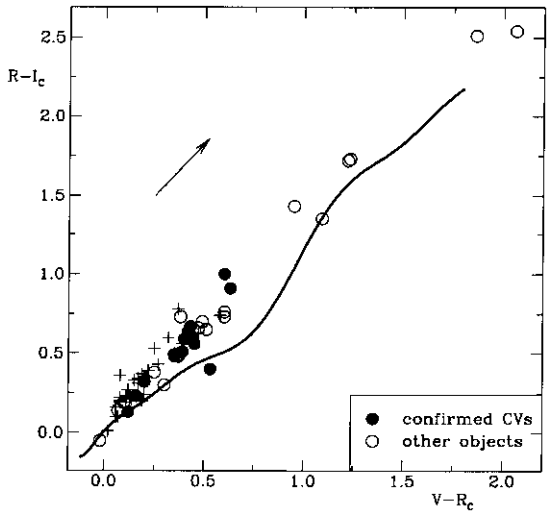

Fig. 2. $V-R_{\rm C}$, $R_{\rm C}-I_{\rm C}$ diagram of programme stars. The solid line is the ZAMS according to Caldwell et al. (1993). No reddening correction has been applied to the data given in Table 6. The reddening vector corresponding to E_{B-V}=0.5 is shown. Legend: *filled circles* = confirmed CVs from the present paper; *open circles* = other programme stars; *plus signs* = validated CVs in quiescence from Papers I and II

PG 1459-026. In the Palomar-Green survey (Green et al. 1986) it is reported at B=15.03, $U-B$=−0.80, $B-V$=+0.11 with multiple spectroscopic observations supporting a CV classification. The DS93 coordinates well match the original PG ones, and the object indicated in their finding chart appears blue on the POSS prints as expected. Thus, everything looks consistent. Yet, our spectrum is that of a M2 V star fainter by 4.2 mag in B (cf. Tables 3 and 6). It seems improbable we observed the wrong star: the stellar pattern around PG 1459-026 is easy to identify and M dwarfs are not so frequent among field stars. Our exposure lasted 40 minutes (cf. Table 1) and to postulate the object was in eclipse when we observed it would imply an unusually long orbital period for a typical CV. A further possibility is that PG 1459-026 is really a CV but it was in an inactive state when we secured the spectrum. Clearly, new observations to solve the issue have to be encouraged.

PG 1520–050. The presence of He II 4686 Å in absorption, while He I lines are absent, suggests a classification as O subdwarf for this faint object at galactic latitude $b=+41°$.

V699 Oph. Howell et al. (1990) obtained CCD images and tried to identify a blue object near the reported position of V699 Oph. They did not find one and did not detected short period term variability by any of the stars in the field. They conclude the star is quite possibly not a CV. Our spectrum is that of a typical K field star and confirms the mis–classification of this object as a CV.

V422 Ara. The blue portion of our spectrum shows an early–A continuum while weak TiO bands corresponding to a K7 V spectral type can be seen in the red part. We measured B=17.7, i.e. 1.5 mag fainter than the reported range of variability. The absence of emission lines suggests none or little interaction in the binary system at the time of our observations. An higher S/N spectrum is required to investigate the profile of Balmer lines in the blue in order to clarify if they come from a WD. The system could be a pre–cataclysmic variable or a CV cought in a very low state of interaction.

V2493 Sgr. There are three stars within 9″ from the marked position of V2493 Sgr in the finding chart of DS93. We obtained spectra of all of them. The spectra of the North (V = 16.3, $B-V$ = +1.55) and East (V = 15.1, $B-V$ = +2.02) components are those of field K7 V stars, while the spectrum of the South–West component is that of an M 3 III star. The presence of weak Hγ and Hδ in emission (and absence of Hβ and Hα) suggests it to be a Mira variable. The spectral tracing in Fig. 7 as well as the values reported in Tables 5 and 6 refer to the Mira.

KY Ara. Our spectrum can be classified as F7 V. The accurate $UBVR_{\rm C}I_{\rm C}$ magnitudes derived by Schaefer & Hoffleit (1994) are nearly identical to our values reported in Table 6. Schaefer & Hoffleit argue for an error in the identification chart of Wyckoff & Wehinger (1978) on which the DS93 chart is based, the true variable having an offset of some arcsec and being fainter than 21 mag in B in 1994.

V3909 Sgr. The probable presence of Hδ in emission could support a classification as Mira variable for this M3 III star.

V3914 Sgr and **V2038 Sgr**. The spectra of these two stars are typical of Mira variables. From the intesity of TiO bands at 6180 and 7100 Å and VO at 7865 Å the spectral types are M7 for V3914 Sgr and M4 for V2038 Sgr.

WW Tel. The spectrum shows a pure absorption continuum similar to a G0 dwarf. This is entirely consistent with the colours reported in Table 6. The B magnitude in our spectrum is close to the minimum brightness reported for this object.

V4019 Sgr. The only lines detected in emission are Hα and Hβ, with an extreme intensity ratio. The flat continuum shows a marked Balmer jump and higher Balmer series line in absorption. The star can be classified as A7e. Adopting a V luminosity class, from the V, $B-V$ values reported in Table 6 a reddening E_{B-V}=0.5 and a distance d=1.2 Kpc can be derived. The reddening is consistent with distance (given the low galactic latitude, $b = -6°$) and suggests a strong interstellar contribution to the intensity of the Na I D absorption line and the large Balmer decrement. Downes et al. (1995) present a higher resolution spectrum over the region 4800−6600 Å which is in strict agreement with ours. They do not exclude the possibility that V4019 Sgr is indeed a CV.

DP Pav. The coordinates reported by DS93 do not match the finding chart. A spectrum of the bright star indicated on the finding chart by DS93 is presented in Fig. 11. Our spectrum can be classified as A2–3 V and the derived B magnitude is comparable with the brighter end of the reported range of variability. Our spectrum however does not look like that of a CV in outburst (cf. UZ Ser in Fig. 16). We also obtained a short exposure of a bright star (α_{2000} = 18h 26m 41.55s, $\delta_{2000} = -64°59'16''$) lying $\sim 1'$ North and $\sim 1'$ West from the South-East corner of the same finding chart, i.e. close to the coordinates cited by DS93. Its spectrum does not resemble that of a CV.

Acknowledgements. We would like to thank the referee (H.W. Duerbeck) for his careful scrutinizing of the manuscript.

References

Barwing H., Schoembs R., 1983, A&A 124, 287
Bessell M.S., 1976, PASP 88, 557
Bond H.E., 1978, PASP 90, 526
Bond H.E., Tifft W.G., 1974, PASP 86, 981
Bruch A., 1984, A&AS 56, 441
Bruch A., Engel A., 1994, A&AS 104, 79, (BE94)
Caldwell J.A.R., Cousins A.W.J., Ahlers C.C., van Wamelen P., Maritz E.J., 1993, South African Astron. Obs. Circulars 15, 1
Downes R., Hoard D.W., Szkody P., Wachter S., 1995, AJ 110, 1824
Downes R.A., Shara M.M., 1993, PASP 105, 127 (DS93)
Duerbeck H.W., 1984, IBVS 2502
Duerbeck H.W., 1987, A Reference Catalogue and Atlas of Galactic Novae. Reidel (D87)
Green R.F., Schmidt M., Liebert J., 1986, ApJS 61, 305
Hartigan P., 1993, AJ 105, 1511
Howell S.T., Szkody P., Kreidl T.J., Mason K.O., Puchnarewicz E.M., 1990, PASP 102, 758
Lamla E., 1982, Landolt-Börnstein Series 2b. In: Schaifers K., Voight H.H. (eds.). Springer, Berlin
Perek L., 1960, Bull. Astron. Inst. Czech. 11, 256
Remillard R.A., Brandt H.V., Brissended R.J.V., et al., 1994, ApJ 428, 785
Schaefer B.E., Hoffleit D., 1994, IBVS 4123
Szkody P., 1994, AJ 108, 639
Wyckoff S., Wehinger P.A., 1978, PASP 90, 557
Zwitter T., Munari U., 1994, A&AS 107, 503 (Paper I)
Zwitter T., Munari U., 1995, A&AS 114, 575 (Paper II)

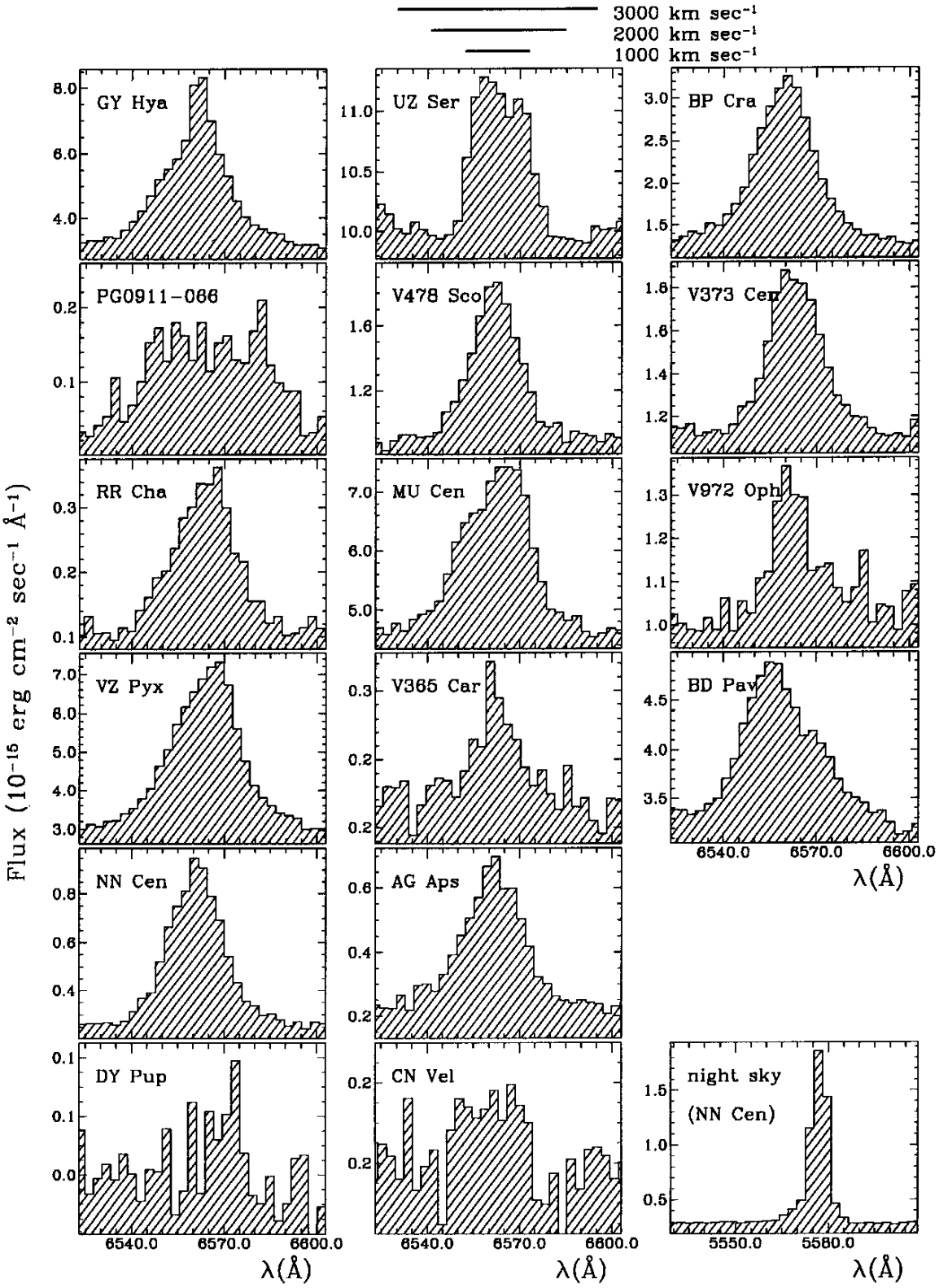

Fig. 3. Hα emission profiles for the validated CVs among the programme stars. Fluxes in units of 10^{-15} erg cm^{-2} s^{-1} Å^{-1}. The night–sky line at 5577.4 Å from the NN Cen spectrum is shown on the same scale as a reference for the instrumental resolution and flux level of the background sky (computed on the same number of CCD columns as for the programme stars)

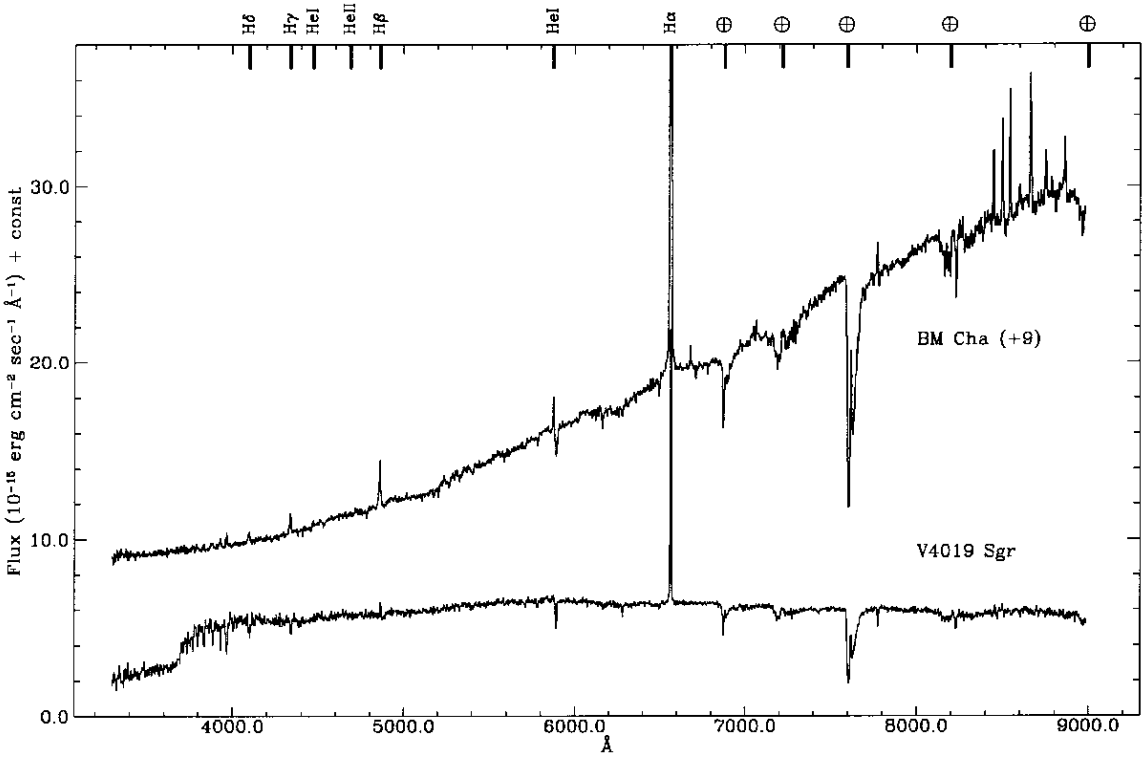

Fig. 4. Spectra of BM Cha and V4019 Sgr. The offset applied for plot clarity is given in brackets next to the star name. The spectra are not corrected for reddening. Fluxes in units of 10^{-15} erg cm^{-2} s^{-1} Å^{-1}

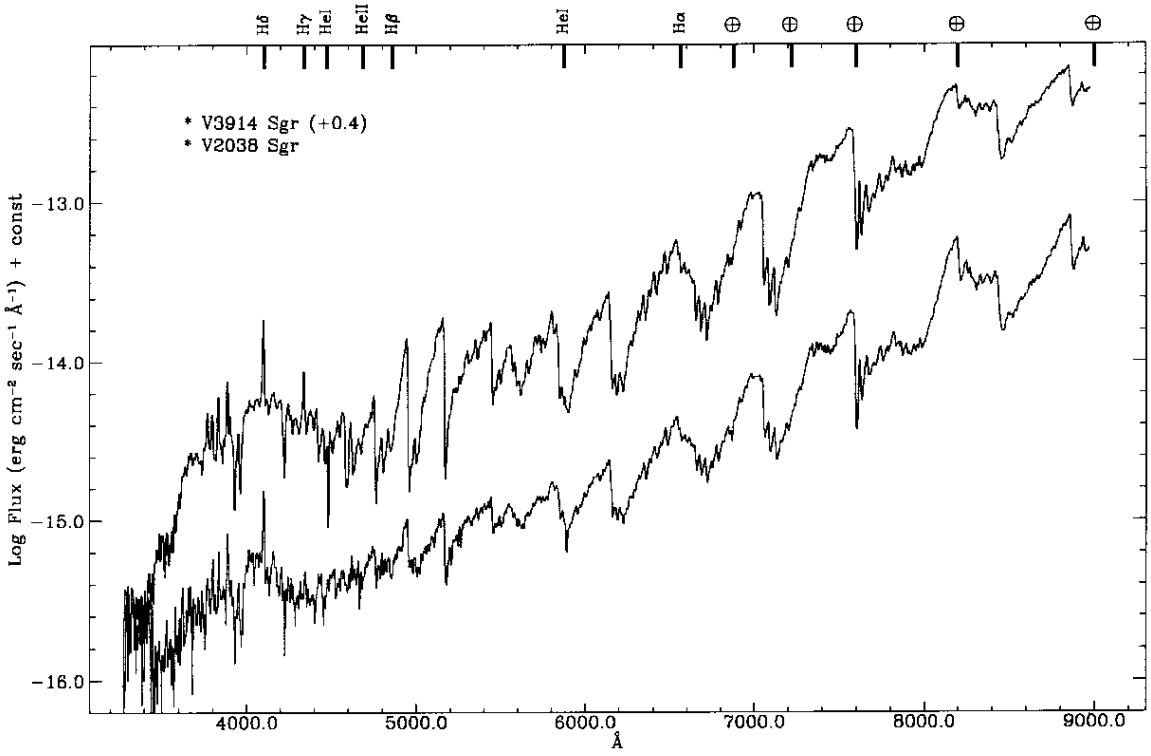

Fig. 5. Spectra of V3914 Sgr and V2038 Sgr. The offset applied for plot clarity is given in brackets next to the star name. The asterisk means that a boxcar smoothing (with a window of 3 pixels) has been applied. The spectra are not corrected for reddening

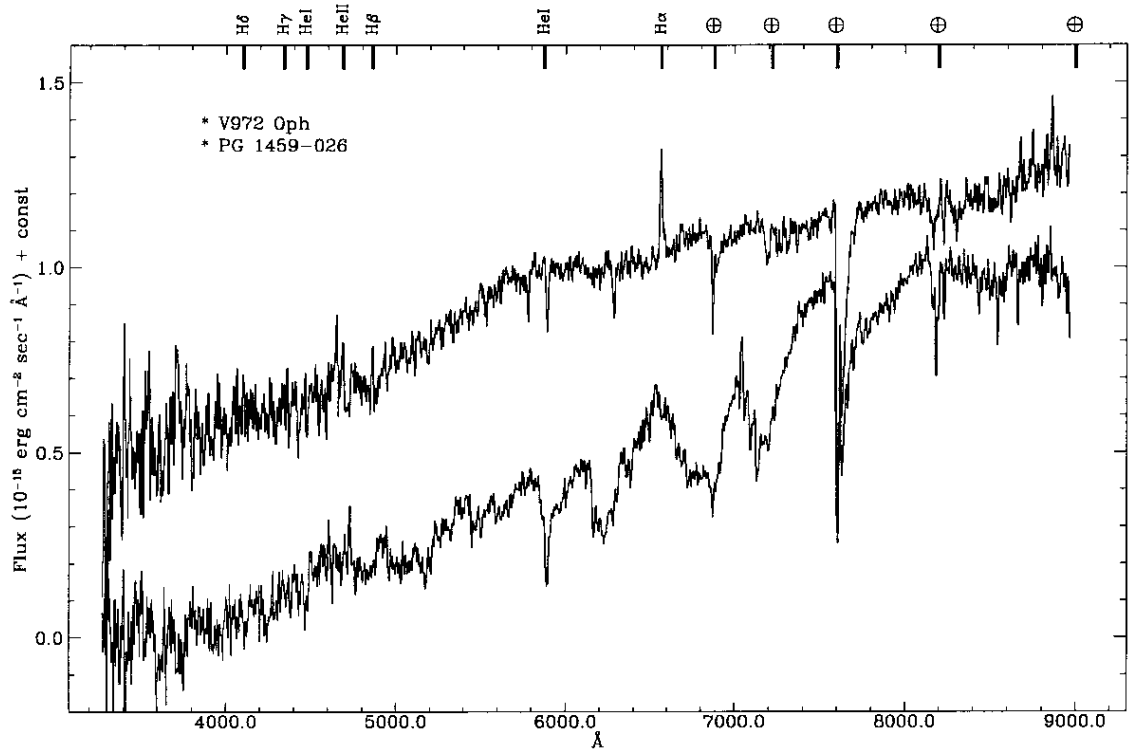

Fig. 6. Spectra of V972 Oph and PG 1459–026. The asterisk means that a boxcar smoothing (with a window of 3 pixels) has been applied. The spectra are not corrected for reddening. Fluxes in units of 10^{-15} erg cm^{-2} s^{-1} Å^{-1}

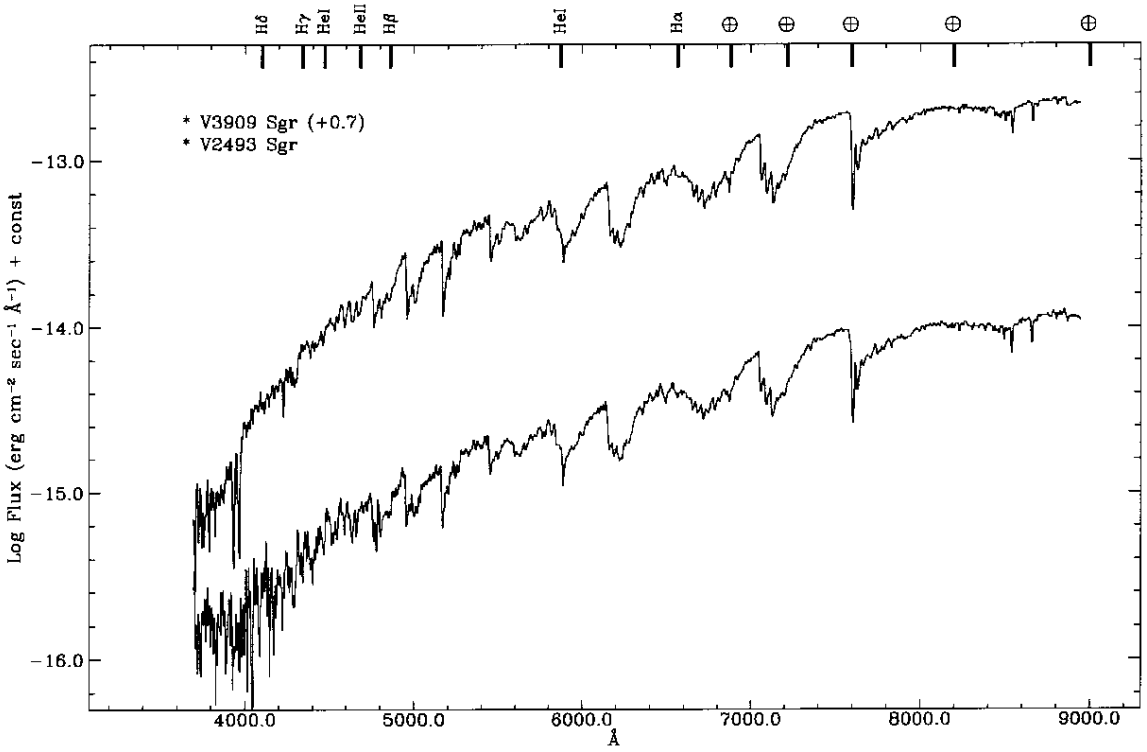

Fig. 7. Spectra of V3909 Sgr and V2493 Sgr. The offset applied for plot clarity is given in brackets next to the star name. The asterisk means that a boxcar smoothing (with a window of 3 pixels) has been applied. The spectra are not corrected for reddening

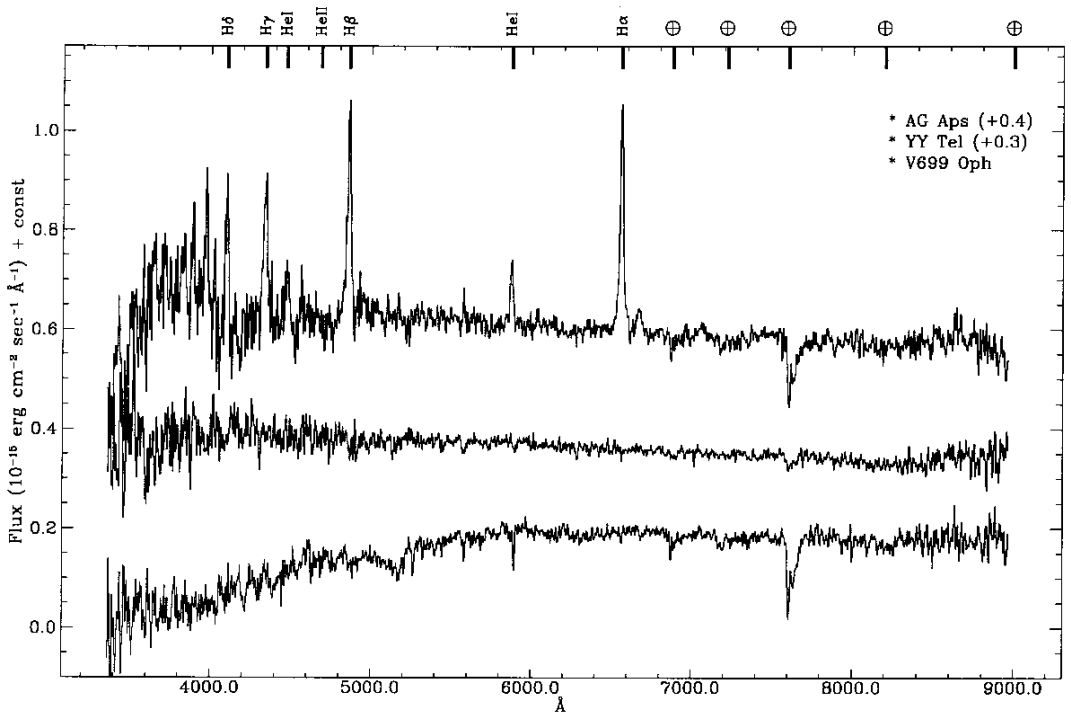

Fig. 8. Spectra of AG Aps, YY Tel and V699 Oph. The offset applied for plot clarity is given in brackets next to the star name. The asterisk means that a boxcar smoothing (with a window of 3 pixels) has been applied. The spectra are not corrected for reddening. Fluxes in units of 10^{-15} erg cm^{-2} s^{-1} Å^{-1}

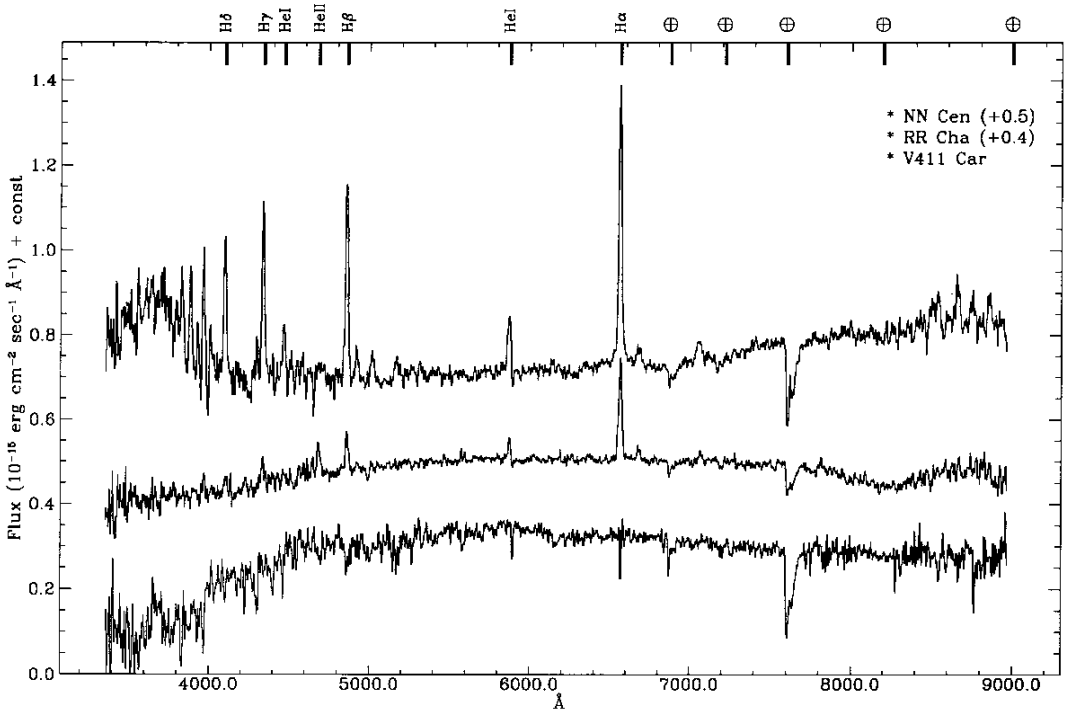

Fig. 9. Spectra of NN Cen, RR Cha and V411 Car. The offset applied for plot clarity is given in brackets next to the star name. The asterisk means that a boxcar smoothing (with a window of 3 pixels) has been applied. The spectra are not corrected for reddening. Fluxes in units of 10^{-15} erg cm^{-2} s^{-1} Å^{-1}

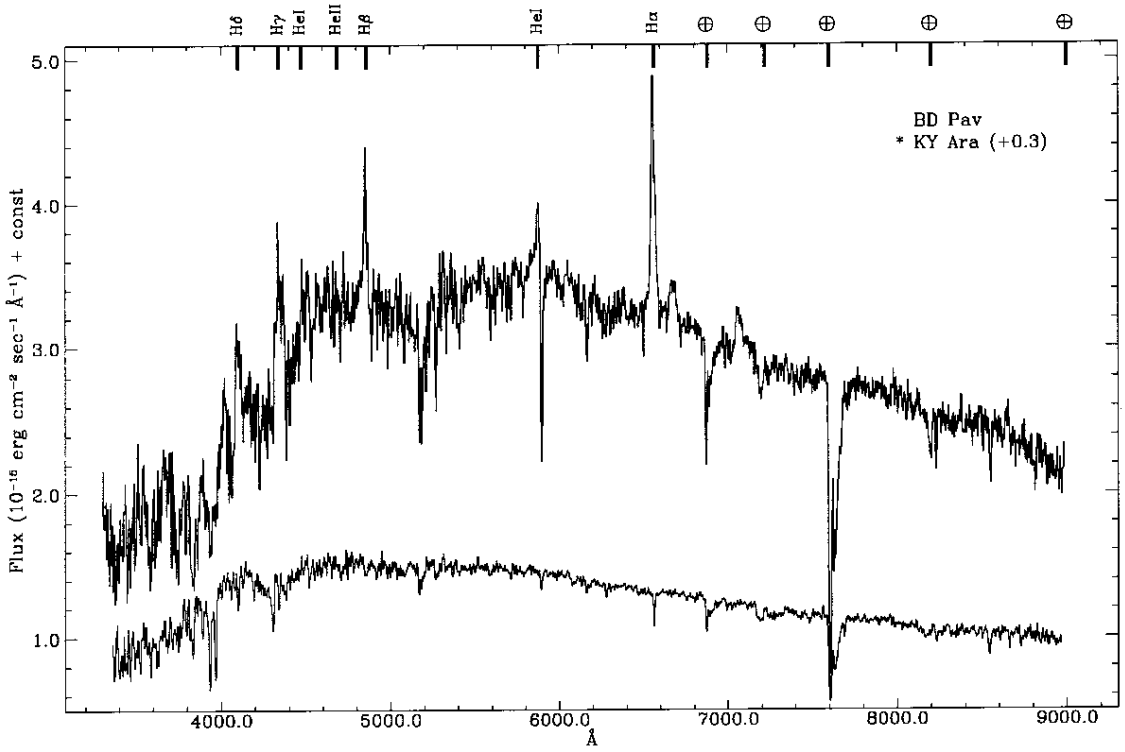

Fig. 10. Spectra of BD Pav and KY Ara. The offset applied for plot clarity is given in brackets next to the star name. The asterisk means that a boxcar smoothing (with a window of 3 pixels) has been applied. The spectra are not corrected for reddening. Fluxes in units of 10^{-15} erg cm^{-2} s^{-1} Å^{-1}

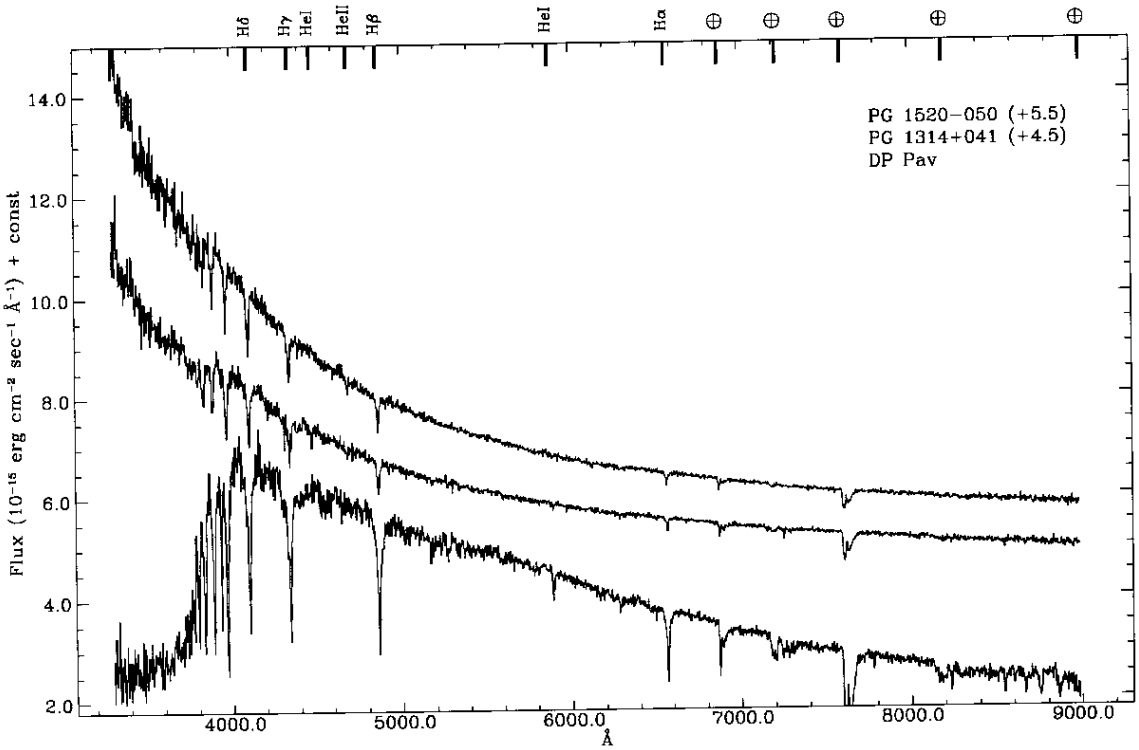

Fig. 11. Spectra of PG 1520–050, PG 1314+041 and DP Pav. The offset applied for plot clarity is given in brackets next to the star name. The spectra are not corrected for reddening. Fluxes in units of 10^{-15} erg cm^{-2} s^{-1} Å^{-1}

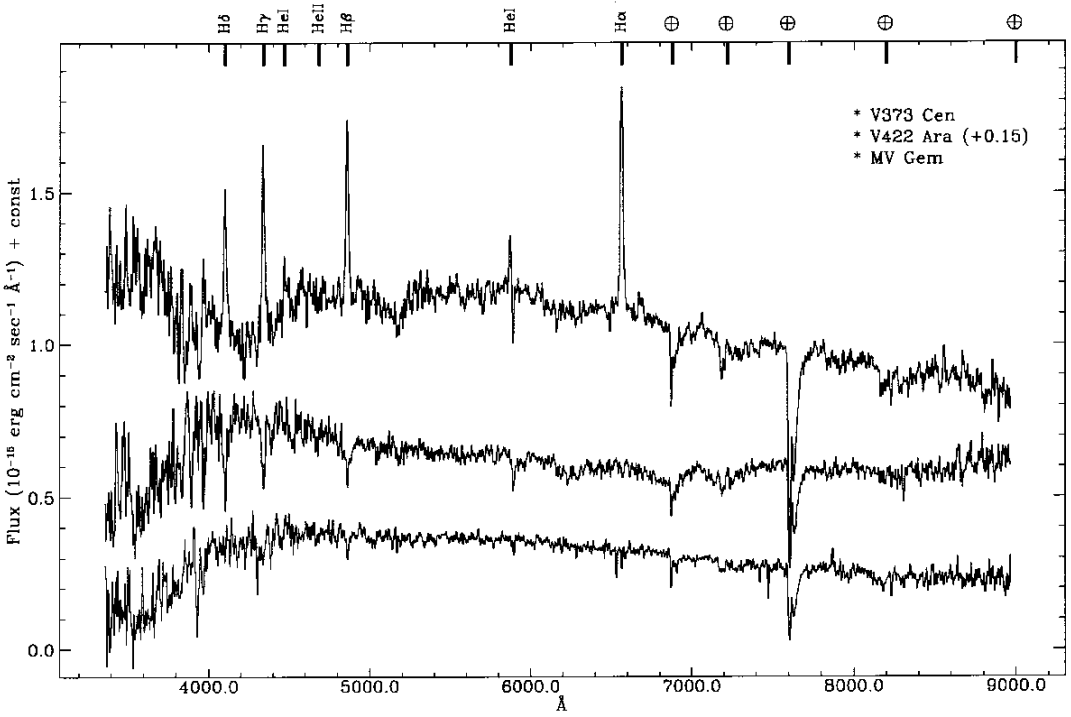

Fig. 12. Spectra of V373 Cen, V422 Ara and MV Gem. The offset applied for plot clarity is given in brackets next to the star name. The asterisk means that a boxcar smoothing (with a window of 3 pixels) has been applied. The spectra are not corrected for reddening. Fluxes in units of 10^{-15} erg cm^{-2} s^{-1} Å^{-1}

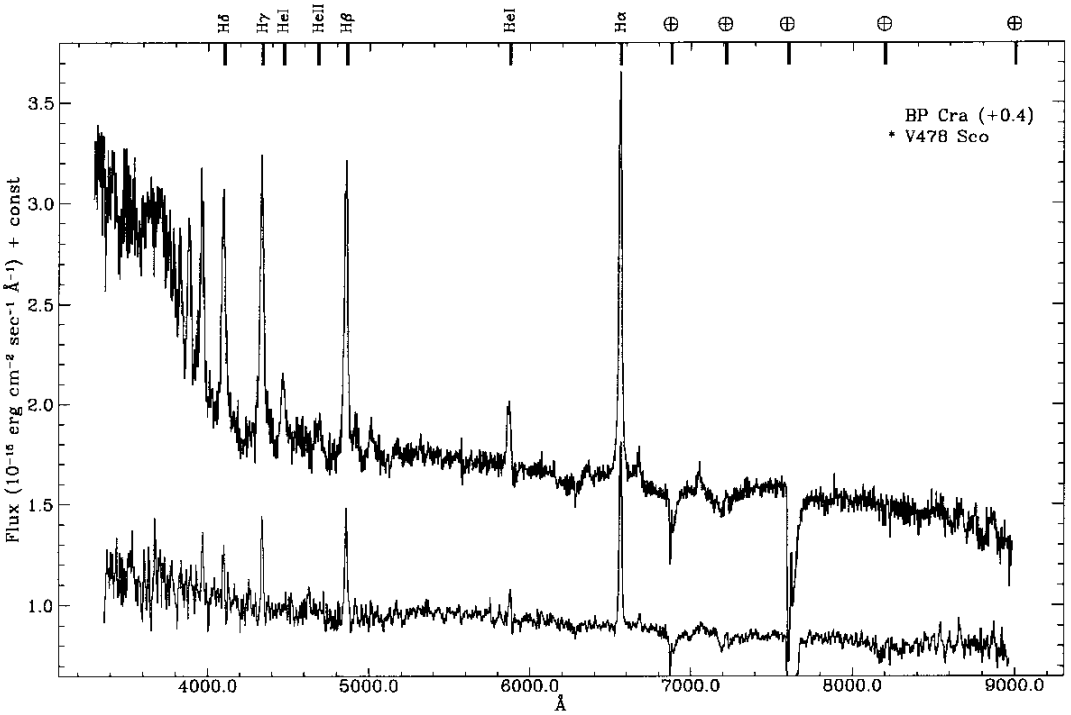

Fig. 13. Spectra of BP Cra and V478 Sco. The offset applied for plot clarity is given in brackets next to the star name. The asterisk means that a boxcar smoothing (with a window of 3 pixels) has been applied. The spectra are not corrected for reddening. Fluxes in units of 10^{-15} erg cm^{-2} s^{-1} Å^{-1}

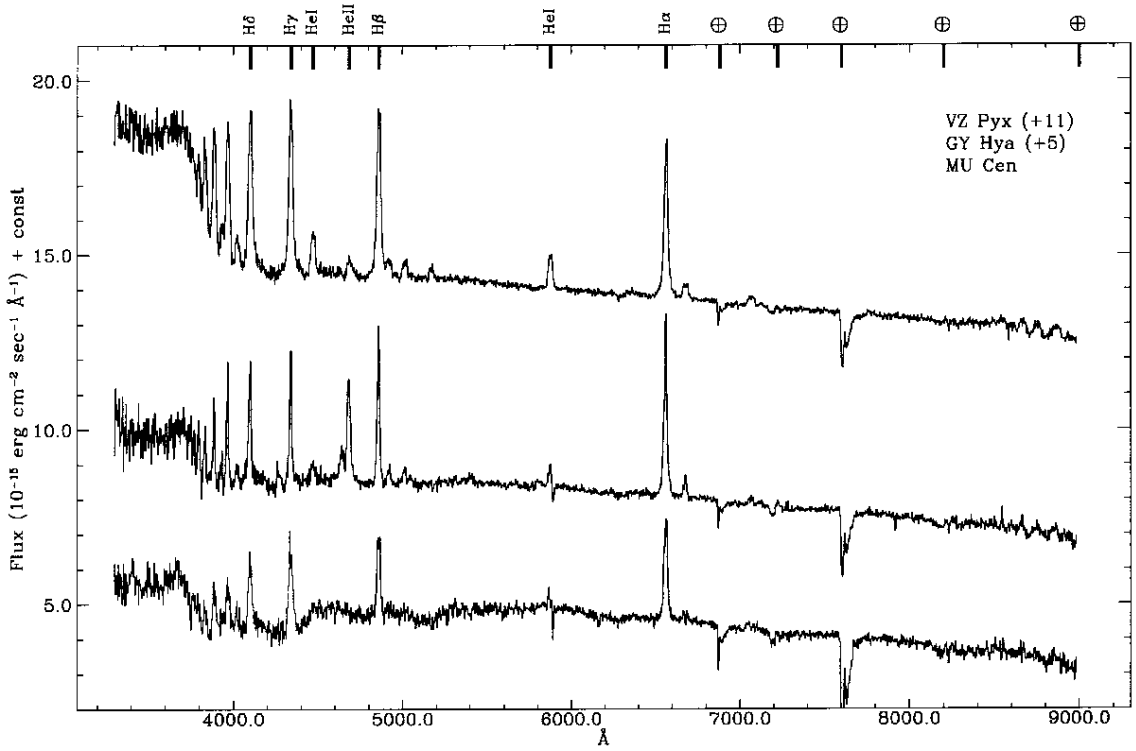

Fig. 14. Spectra of VZ Pyx, GY Hya and MU Cen. The offset applied for plot clarity is given in brackets next to the star name. The spectra are not corrected for reddening. Fluxes in units of 10^{-15} erg cm^{-2} s^{-1} Å^{-1}

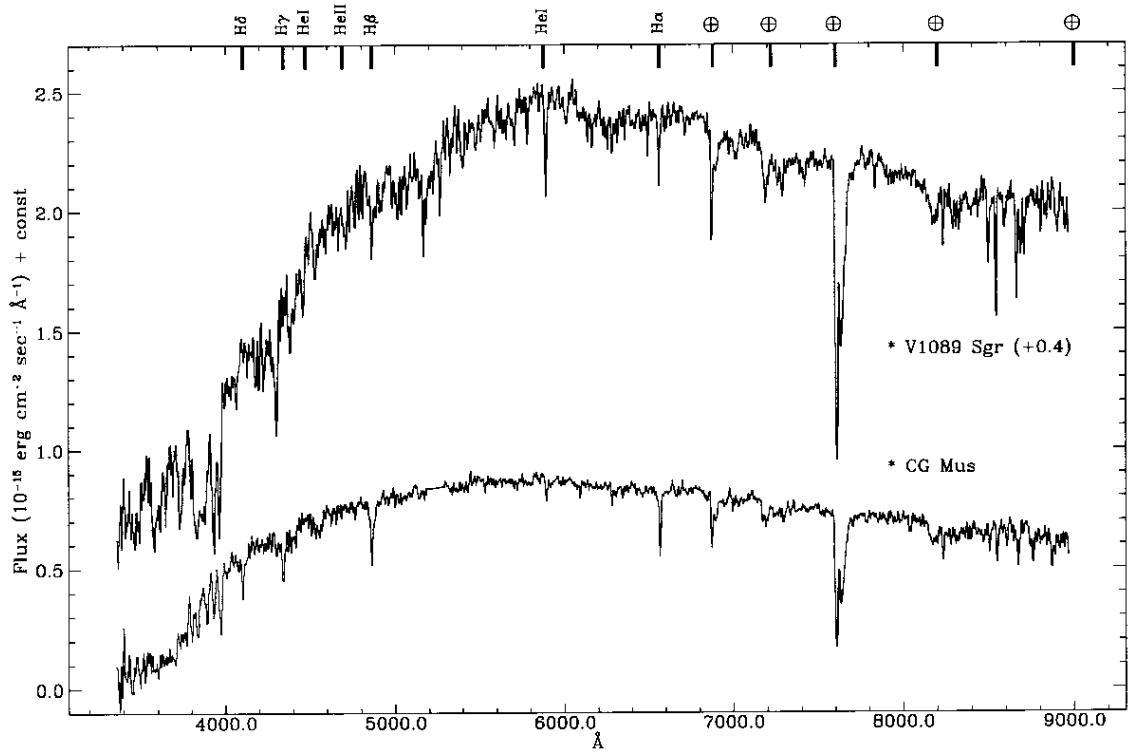

Fig. 15. Spectra of V1089 Sgr and CG Mus. The offset applied for plot clarity is given in brackets next to the star name. The asterisk means that a boxcar smoothing (with a window of 3 pixels) has been applied. The spectra are not corrected for reddening. Fluxes in units of 10^{-15} erg cm^{-2} s^{-1} Å^{-1}

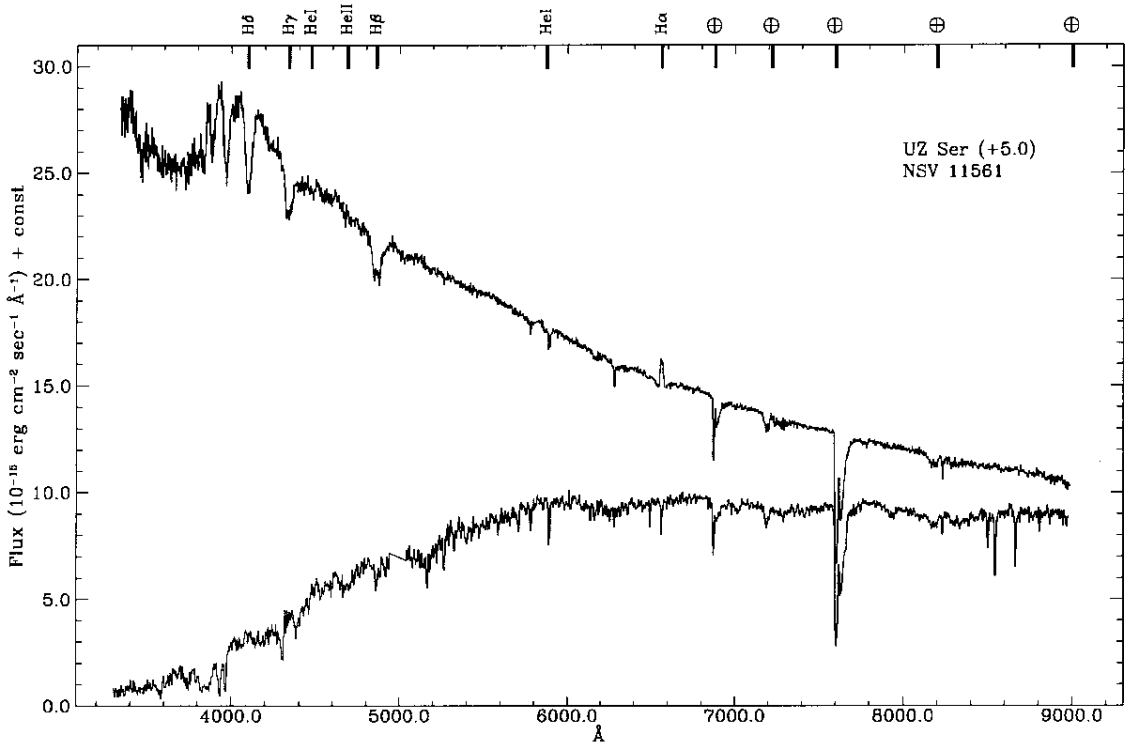

Fig. 16. Spectra of UZ Ser and NSV 11561. The offset applied for plot clarity is given in brackets next to the star name. The spectra are not corrected for reddening. Fluxes in units of 10^{-15} erg cm^{-2} s^{-1} Å^{-1}

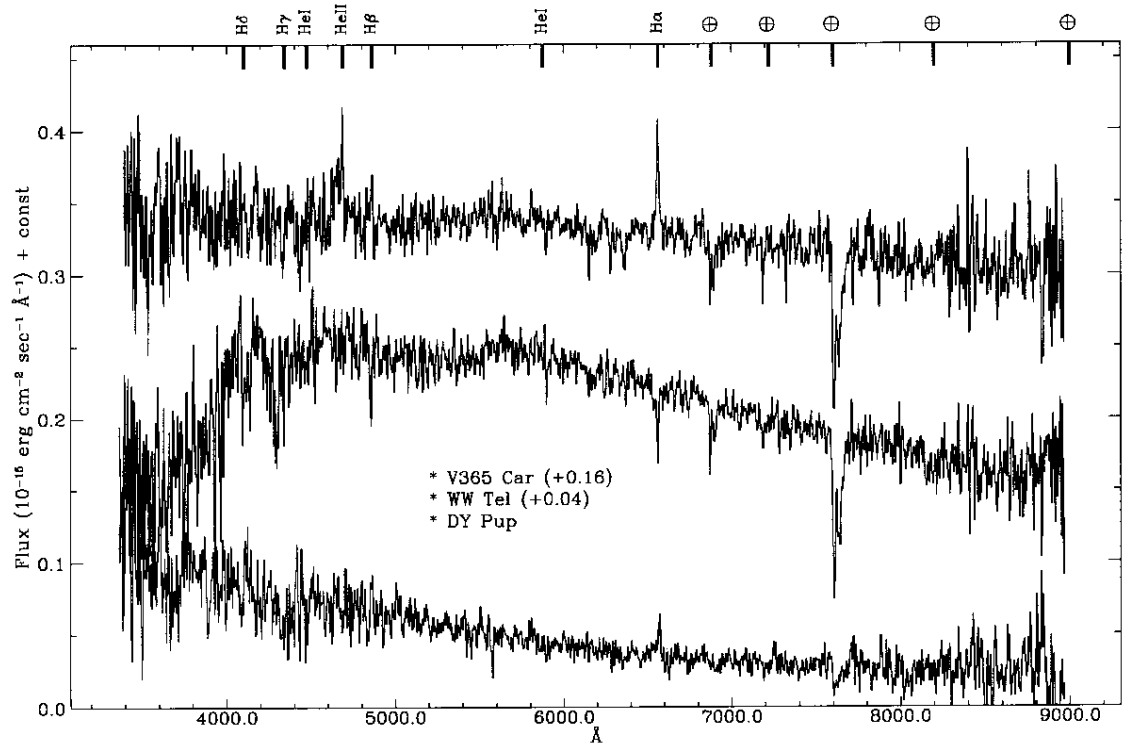

Fig. 17. Spectra of V365 Car, WW Tel and DY Pup. The offset applied for plot clarity is given in brackets next to the star name. The asterisk means that a boxcar smoothing (with a window of 3 pixels) has been applied. The spectra are not corrected for reddening. Fluxes in units of 10^{-15} erg cm^{-2} s^{-1} Å^{-1}

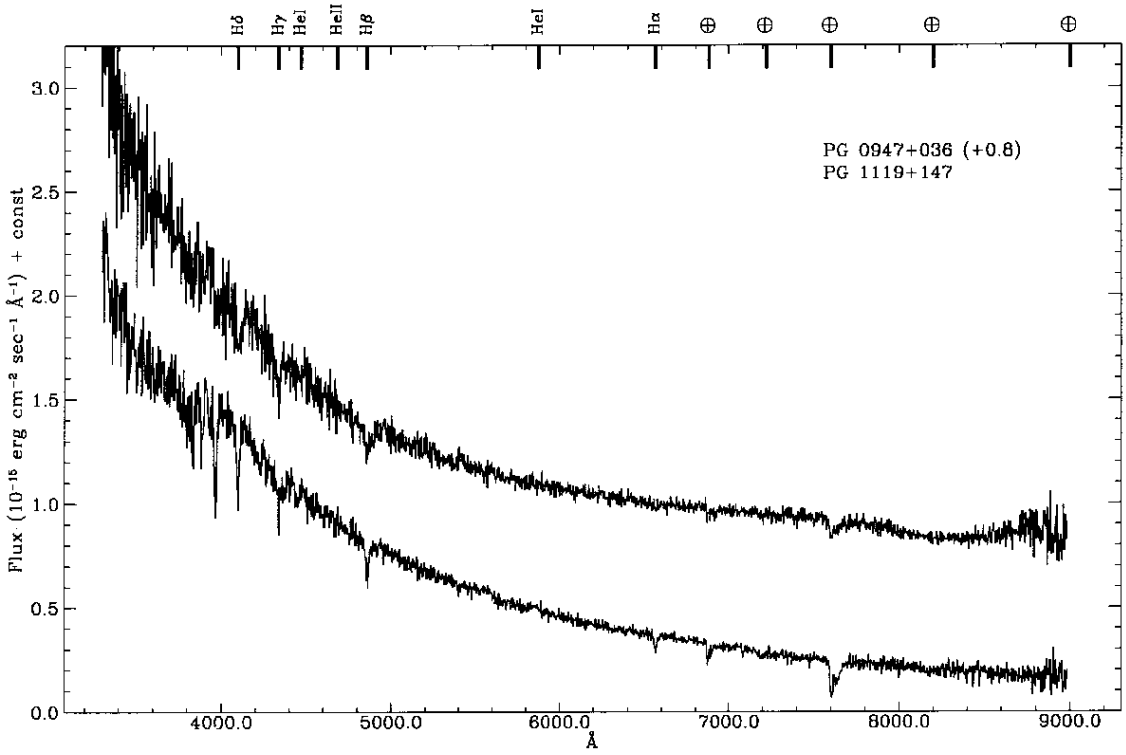

Fig. 18. Spectra of PG 0947+036 and PG 1119+147. The offset applied for plot clarity is given in brackets next to the star name. The spectra are not corrected for reddening. Fluxes in units of 10^{-15} erg cm^{-2} s^{-1} Å^{-1}

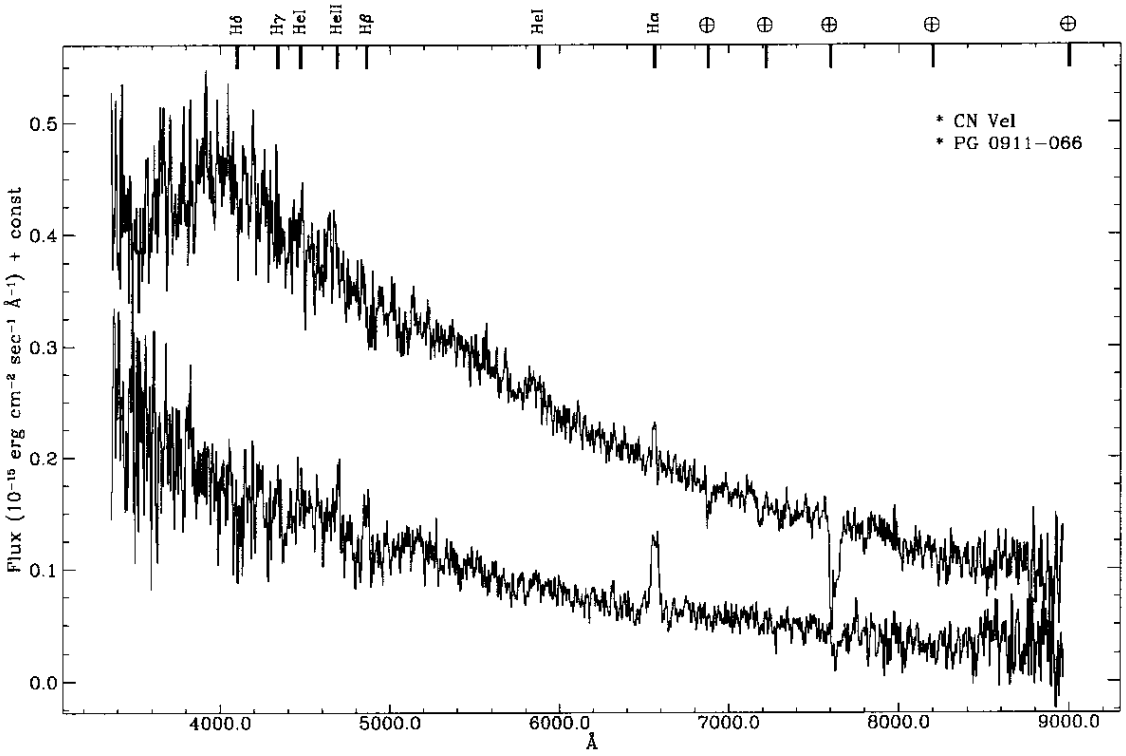

Fig. 19. Spectra of CN Vel and PG 0911–066. The spectra are not corrected for reddening. Fluxes in units of 10^{-15} erg cm^{-2} s^{-1} Å^{-1}